

Magnetic-Field-Induced Suppression of Electronic Conduction in a Superlattice

A. Patanè,^{1,*} N. Mori,² D. Fowler,¹ L. Eaves,¹ M. Henini,¹ D. K. Maude,³ C. Hamaguchi,² and R. Airey⁴

¹*School of Physics and Astronomy, University of Nottingham, NG7 2RD, United Kingdom*

²*Department of Electronic Engineering, Osaka University, Suita City, Osaka 565-0871, Japan*

³*Grenoble High Magnetic Field Laboratory, MPI-CNRS, F-38042 Grenoble, France*

⁴*Department of Electronic and Electrical Engineering, University of Sheffield, S3 3JD Sheffield, United Kingdom*

(Received 4 March 2004; published 29 September 2004)

We use a magnetic field applied along the axis of a semiconductor superlattice (SL) as a controllable means of creating a one-dimensional band structure. We demonstrate that the current flow through the SL is strongly suppressed when the electron motion perpendicular to the SL axis is strongly confined by the quantizing magnetic field. By modeling this behavior using semiclassical and nonequilibrium Green's function methods, we show that the observed quenching arises from a qualitative change in electron dynamics caused by increasing quantum confinement.

DOI: 10.1103/PhysRevLett.93.146801

PACS numbers: 73.21.Cd, 72.10.-d, 72.80.Ey

The multilayered superlattice (SL) heterostructure [1] provides the condensed matter physicist with a system in which a highly anisotropic electronic band structure can be “made to order.” For example, it has been used as a testbed for the study of fundamental quantum phenomena, such as carrier localization effects in the electrical conduction of one-dimensional (1D) disordered systems [2] and Bloch oscillations [3–5]. The SL concept is also a key component in novel device structures, such as quantum cascade lasers [6,7]. The electronic properties of a SL can be controlled in a flexible way by varying the miniband width Δ and the extent of the minizone in k space. The extent of the minizone is simply $2\pi/d$, where d is the SL period. The miniband width is mainly determined by the rate at which an electron tunnels between adjacent quantum wells (QWs) and can be adjusted by changing the thickness and composition of the wells and tunnel barriers. This also determines the extent of carrier confinement along the SL axis. In the limit of small Δ , the electrons undergo free planar motion in a series of uncoupled QWs. Nanometer-scale quantum pillars fabricated by lithography and etching techniques [8] could in principle provide a means of confining the carrier motion in the SL plane to create a 1D conduction band. However, this approach is presently limited by technological constraints on the control of the pillar width at length scales, 100 nm or less, necessary for observing quantum effects in this type of structure.

In this work, we create a quasi-1D band structure by applying a large quantizing magnetic field B (up to 23 T) along the SL axis such that the cyclotron energy $\hbar\omega_c$ exceeds Δ . We demonstrate that the SL current is strongly quenched at high B and low temperature and that plots of the current intensity versus the ratio $\hbar\omega_c/\Delta$ for SLs with different Δ fall approximately on a single “universal” curve. We analyze this behavior using a nonequilibrium Green's function (NEGF) method of the type developed by Wacker and co-workers [9,10] but extended to include

the effect of the quantizing magnetic field. We demonstrate that the current quenching arises from the quasi-1D SL states formed in the quantum limit. This study is relevant to the understanding of magnetoresistance effects reported previously in semiconductor SLs [11–13]. Also, it is of general interest as it concerns the motion of electrons in a quasi-1D periodic potential and the fundamental changes in electron dynamics caused by increasing quantum confinement [14]. This is of topical interest for the properties of other anisotropic conductors, such as graphitic materials and organic crystals, which are presently attracting great interest in the condensed matter physics community.

We investigated a number of SLs with different unit cell structures and differently designed interfaces between the n -type contact layers and the SL array. A Kronig-Penney model was used to determine Δ . In this Letter, we focus on three samples $S1$, $S2$, and $S3$, with the following values of Δ : 12 meV ($S1$); 20 meV ($S2$); 30 meV ($S3$). They were grown by molecular beam epitaxy on (100)-oriented Si-doped n -type (10^{18} cm $^{-3}$) substrates. Samples $S1$ and $S3$ contain 15 SL periods, which are separated from two heavily n -doped GaAs contacts by Si-doped Al $_{0.03}$ Ga $_{0.97}$ As ($S1$) or Al $_{0.06}$ Ga $_{0.94}$ As ($S3$) layers of width 30 nm and doping concentration of 2×10^{16} and 6×10^{16} cm $^{-3}$, respectively. A SL unit cell is formed by 2.5 nm of Al $_{0.3}$ Ga $_{0.7}$ As and 10 nm ($S1$) or 6.5 nm ($S3$) of GaAs doped with Si at 1.8×10^{16} cm $^{-3}$. Sample $S2$ contains 15 SL periods, which are separated from two heavily n -doped GaAs contacts by Si-doped GaAs layers of width 50 nm and doping concentration of 1×10^{17} cm $^{-3}$. Each unit cell of the SL is formed by a 1 nm AlAs layer, a 7 nm QW layer of GaAs, and an InAs layer of thickness of 0.8 monolayers inserted at the center of each QW, all doped with Si at 3×10^{16} cm $^{-3}$. The samples were processed into circular mesa devices of diameter 25 μ m, with Ohmic contacts to the substrate and top capping layer.

Our SLs were designed so that the low-energy k states of the lowest energy miniband were aligned with the Fermi energy of the doped contact layers at zero bias. This ensures a small and Ohmic contact impedance, which is insensitive to the effect of B . For devices in which the chemical potential of the electrons in the doped contact emitter layer lies below the energy of the SL, the magnetic field leads to a strong suppression of the SL current due to a decrease in the rate of injection of electrons into the SL miniband from the emitter states [15]. For samples $S1$ and $S3$, the alignment of the chemical potential was achieved by increasing the conduction band energy of the doped GaAs contact layers by the addition of a small percentage of Al. For sample $S2$, we achieved alignment by incorporating an InAs layer at the center of each GaAs QW of the SL unit cells [16].

Figure 1 shows the B dependence of the current-voltage plots, $I(V)$, at 4.2 K for all SLs. At $B = 0$ T, the $I(V)$ curves exhibit an Ohmic region at low bias, followed by a peak in the current and a region of negative differential conductance (NDC), in which occurs small steplike features associated with the formation of charge domains [17]. The current is suppressed by the application of the

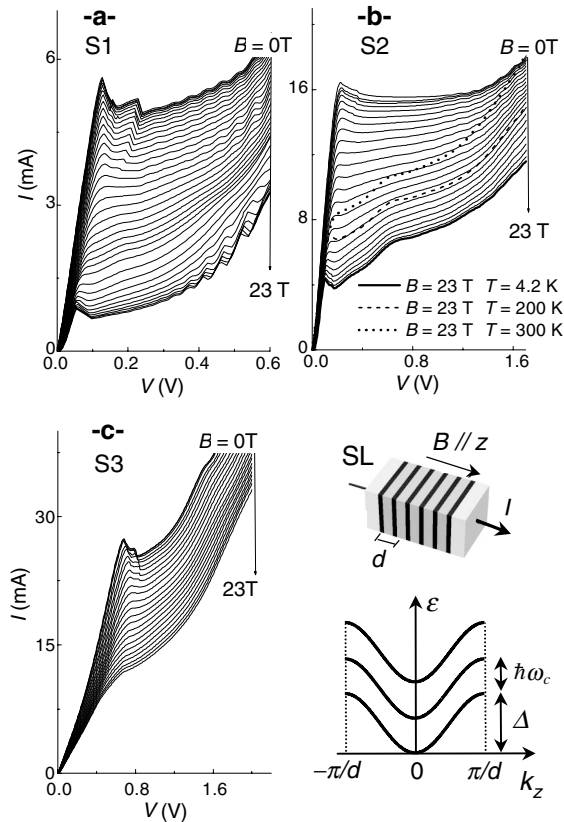


FIG. 1. $I(V)$ curves versus B for samples $S1$ (a), $S2$ (b), and $S3$ (c) at $T = 4.2$ K. B is increased from 0 to 23 T by steps of 0.5 T ($S1$) or 1 T ($S2$ and $S3$). The thick lines in (b) represent $I(V)$ curves at $B = 23$ T and at different temperatures. The inset sketches the geometry of our experiment and the SL Landau level minibands.

magnetic field. When the intensity of the current peak in $I(V)$ is plotted versus the ratio $\hbar\omega_c/\Delta$, we find that the data for all the SLs fall approximately on a single universal curve (see Fig. 2). Similar curves were obtained also by plotting the dependence of current measured at lower voltages. In contrast, at higher voltages, the current has a weaker B dependence due to magnetophonon resonance effects [11–13,18]. In this Letter, we focus on the low-bias regime.

To understand the B -induced quenching of current, we first consider a semiclassical model for electron motion. At $B = 0$ T, electrons are accelerated by the electric field, F , and scattered by impurities, well width fluctuations, and phonons [19,20], resulting in an overall drift motion along the SL axis. Provided that the average scattering time τ is much smaller than ω_B^{-1} , where $\omega_B = eFd/\hbar$ is the Bloch frequency, the wave vector (k) of electrons remains within the range 0 to $\pi/(2d)$, where the velocity increases with k . In this regime, an increase of F leads to an increasing average drift velocity and a linear increase of current. In contrast, when $\tau > \omega_B^{-1}$, electrons reach the region of k for which an increase of k decreases the mean velocity, thus producing a region of NDC in $I(V)$. The drift velocity-field characteristic is given by $v = 2v_p\omega_B\tau/[1 + (\omega_B\tau)^2]$, where v_p is the peak drift velocity and τ includes inelastic (τ_i) and elastic (τ_e) scattering processes, i.e., $\tau^{-1} = \sqrt{\tau_i^{-1}(\tau_i^{-1} + \tau_e^{-1})}$ [19]. According to this model, the miniband conduction is totally quenched in the absence of inelastic scattering, i.e., $v \rightarrow 0$ as $\tau_i \rightarrow \infty$, and/or in the presence of strong elastic scattering, i.e., $v \rightarrow 0$ as $\tau_e \rightarrow 0$. The scattering mechanisms and the drift velocity are modified by the magnetic field. As shown in Fig. 2(b), for $\hbar\omega_c < \Delta$, the energies of the quasi-1D Landau level minibands overlap with each other and elastic and inelastic scattering processes involving a change of the Landau index N can occur. In contrast, for $\hbar\omega_c > \Delta$, the minibands become energetically decoupled from each other. Since Δ is smaller than the longitudinal optical (LO) phonon energy, $\hbar\omega_{LO}$, for all three SLs, optical-phonon scattering processes are forbidden within a Landau level miniband with $\tau_i \rightarrow \infty$. In this regime, electrons can only undergo elastic processes and/or quasielastic scattering by acoustic phonons within one Landau miniband. This leads to a continuous reversal of the electron velocity and to a corresponding suppression of the SL current.

The similarity in the B -induced quenching of the miniband conduction observed in SLs with different Δ is indicative of the formation of 1D Landau level minibands when $\hbar\omega_c > \Delta$ and of the corresponding change in inelastic scattering. At these high B , the SL current is only partly restored with increasing the sample temperature up to 300 K [see Fig. 1(b)]. This temperature dependence, which differs from the thermal decrease of the SL current observed at $B = 0$ T in our SLs and in other similar SLs reported in the literature [21], indicates a slight increase

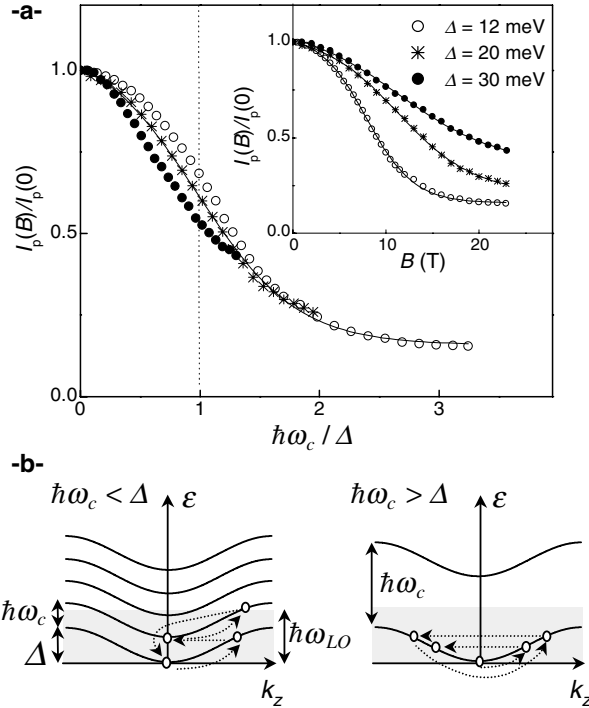


FIG. 2. (a) Dependence of I_p on $\hbar\omega_c/\Delta$ and B for our SLs ($T = 4.2$ K). Continuous lines are guides to the eye. (b) Sketch of elastic and inelastic collisions for $\hbar\omega_c < \Delta$ and $\hbar\omega_c > \Delta$.

in efficiency of inelastic phonon scattering processes due to the thermal population of higher Landau energy minibands.

In contrast to the sharp falloff of the current when $\hbar\omega_c = \Delta$ predicted by semiclassical Monte Carlo simulations of the electron motion [22], the measured current is quenched gradually as B is increased beyond the $\hbar\omega_c = \Delta$ condition. This suggests that the Landau level minibands are energy broadened so that overlap occurs even when $\hbar\omega_c > \Delta$. Also the applied electric field tends to localize the miniband states into Wannier-Stark (WS) states [23,24]. In the WS quantization regime, Landau levels associated with WS states localized at different QWs can have the same energy even when $\hbar\omega_c > \Delta$, thus allowing elastic and inelastic inter-QW scattering processes involving a change of the Landau index N [25–27]. To understand how these phenomena affect the current quenching, we model the miniband conduction by a transport theory that combines both quantum effects and scattering events; i.e., we use a NEGF method of the type developed by Wacker and co-workers [9,10] but extended to include the effect of the quantizing magnetic field.

We describe the electron motion along the SL axis z by using the set of Wannier functions

$$\Psi(z - Md) = \sqrt{\frac{d}{2\pi}} \int_{-\pi/d}^{\pi/d} e^{-iMkd} \phi_k(z) dk, \quad (1)$$

where M is the Wannier index and $\phi_k(z)$ is a SL miniband

Bloch state. The electronic states including the xy motion are specified by the Landau index N , the guiding coordinate X , and the Wannier index M . Since the Wannier functions are localized within single QWs, we consider a local scattering model in which we neglect scattering matrix elements between nonadjacent QWs and determine the current from the M to the $(M + 1)$ well according to the relation

$$\begin{aligned} J^{M \rightarrow M+1} &= \frac{4eT_1}{\hbar} \sum_{NX} \text{Re}\{i\langle a_{NXM}^+(t) a_{NXM+1}(t) \rangle\} \\ &= \frac{eT_1}{\pi\hbar l_B^2} \sum_N \int \text{Re} G_{M+1,M}^<(N; E) dE, \quad (2) \end{aligned}$$

where a_{NXM} (a_{NXM}^+) is the annihilation (creation) operator for the Wannier-Landau (WL) basis state $|N, X, M\rangle$ with associated energy $E_{NM} = (N + 1/2)\hbar\omega_c - MeFd$, T_1 is the interwell coupling strength, l_B is the magnetic length,

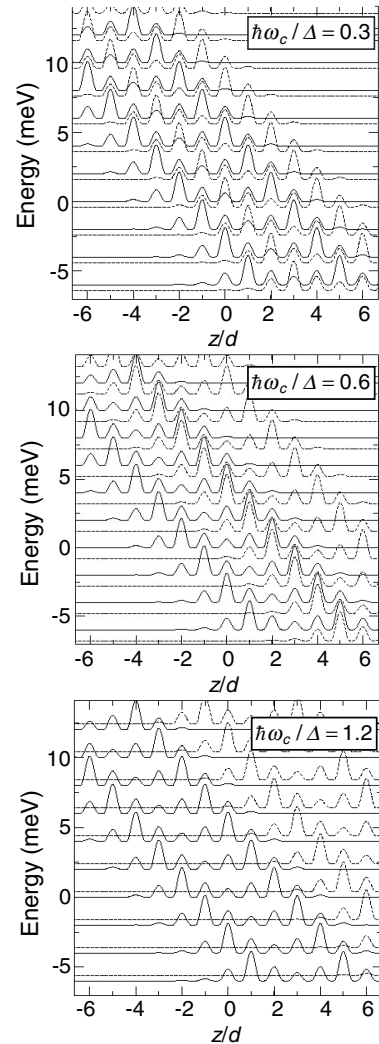


FIG. 3. Probability densities of the Wannier-Landau wave functions for the first ($N = 0$, continuous curves) and second ($N = 1$, dotted curves) Landau level at different values of $\hbar\omega_c/\Delta$ for $\Delta = 12$ meV and $eFd = 2$ meV.

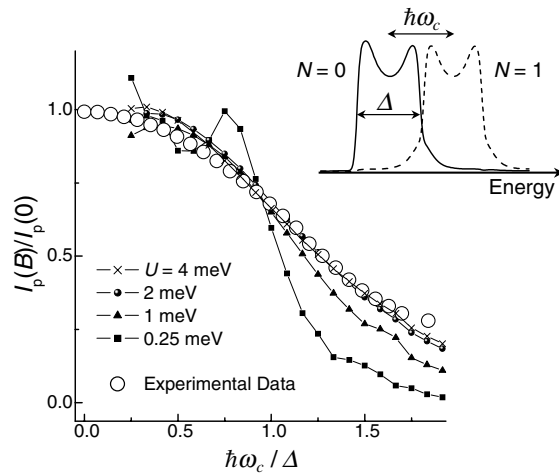


FIG. 4. Comparison between the measured dependence of I_p on $\hbar\omega_c < \Delta$ for sample S1 ($\Delta = 12$ eV) and that calculated according to the NEGF model for different values of U ($T = 4.2$ K). The inset sketches the density of states for the first two SL Landau level minibands.

and $G_{M_1 M_2}^<(N; E)$ is the lesser Green's function, which can be calculated via the Keldysh equation [28]. We consider short-range elastic scattering events and a constant scattering potential U ; we describe the optical-phonon scattering by a Fröhlich coupling constant, $\alpha = 0.07$, and a phonon energy, $\hbar\omega_{LO} = 36.6$ meV; for acoustic phonon scattering, we assume a continuous linear dispersion and longitudinal speed of sound $s_l = 5.2 \times 10^3$ m/s.

As shown in Fig. 3, the overlap between different WL levels decreases smoothly as B increases. This reduces the scattering matrix element connecting Wannier states of different QWs and hence suppresses the electrical conduction. Figure 4 shows the calculated B dependence of I for various values of the scattering potential U and $\Delta = 12$ meV. The NEGF model describes well the measured B dependence of I for $U > 1$ meV. Increasing U leads to a smoother current quenching due to an increasing probability of elastic scattering-induced inter-Landau level tunneling. In a miniband picture, this effect can be understood in terms of the energy broadening of the Landau minibands, which gives rise to an overlap between the minibands even when $\hbar\omega_c > \Delta$ (see inset of Fig. 4), thus freeing the electrons from the constraint of scattering within a single miniband only.

In conclusion, we have created a 1D band structure by applying a large quantizing magnetic field along the axis of a semiconductor SL. This acts to suppress the electrical conduction. Using semiclassical and NEGF methods, we demonstrated that this behavior arises from the quasi-1D SL states formed in the quantum limit and from the

restricted range of scattering processes available to the conduction electrons. Our study of these artificial “tailor made” conductors demonstrates the fundamental change in electrical properties caused by increasing quantum confinement.

We acknowledge the support of the Engineering and Physical Sciences Research Council (United Kingdom).

*Electronic address: Amalia.Patane@nottingham.ac.uk

- [1] L. Esaki and R. Tsu, IBM J. Res. Dev. **14**, 61 (1970).
- [2] V. Bellani *et al.*, Phys. Rev. Lett. **82**, 2159 (1999).
- [3] J. Feldman *et al.*, Phys. Rev. B **46**, 7252 (1992).
- [4] Y. Shimada *et al.*, Phys. Rev. Lett. **90**, 046806 (2003).
- [5] P.G. Savvidis, B. Kolasa, G. Lee, and S.J. Allen, Phys. Rev. Lett. **92**, 196802 (2004).
- [6] J. Faist *et al.*, Science **264**, 553 (1994).
- [7] R. Kohler *et al.*, Nature (London) **417**, 156 (2002).
- [8] M.T. Bjork *et al.*, Appl. Phys. Lett. **80**, 1058 (2002).
- [9] A. Wacker and A.P. Jauho, Phys. Rev. Lett. **80**, 369 (1998).
- [10] A. Wacker *et al.*, Phys. Rev. Lett. **83**, 836 (1999).
- [11] H. Noguchi, H. Sakaki, T. Takamasu, and N. Miura, Phys. Rev. B **45**, 12 148 (1992).
- [12] P. Gassot *et al.*, Phys. Rev. B **54**, 14 540 (1996).
- [13] Yu. A. Pusep *et al.*, Phys. Rev. B **68**, 195207 (2003).
- [14] H. Sakai, Jpn. J. Appl. Phys. **19**, L735 (1980).
- [15] A.A. Krokhin *et al.*, Phys. Rev. B **63**, 195323 (2001).
- [16] A. Patanè *et al.*, Appl. Phys. Lett. **81**, 661 (2002).
- [17] For details, see H.T. Grahn, *Semiconductor Superlattices: Growth and Electronic Properties* (World Scientific, Singapore, 1995); K. Leo, *High-Field Transport in Semiconductor Superlattices* (Springer-Verlag, Berlin, 2003); F.-J. Niedernostheide, *Nonlinear Dynamics and Patterns Formation in Semiconductors and Devices* (Springer, Berlin, 1995).
- [18] R. Ferreira, Phys. Rev. B **43**, 9336 (1991).
- [19] A. A. Ignatov, E. P. Dodin, and V. I. Shashkin, Mod. Phys. Lett. **5**, 1087 (1991).
- [20] E. Diez, F. Dominguez-Adame, and A. Sanchez, Microelectron. Eng. **43**, 117 (1998).
- [21] G. Brozak *et al.*, Phys. Rev. Lett. **64**, 3163 (1990).
- [22] N. Mori, C. Hamaguchi, L. Eaves, and P.C. Main, Physica (Amsterdam) **298B**, 329 (2002).
- [23] J. Bleuse, G. Bastard, and P. Voisin, Phys. Rev. Lett. **60**, 220 (1988).
- [24] E. E. Mendez, F. Agulló-Rueda, and J.M. Hong, Phys. Rev. Lett. **60**, 2426 (1988).
- [25] W. Müller, H.T. Grahn, R.J. Haug, and K. Ploog, Phys. Rev. B **46**, 9800 (1992).
- [26] F. Piazza, L. Pavesi, H. Cruz, M. Micovic, and C. Mendoca, Phys. Rev. B **47**, 4644 (1993).
- [27] K. Kempa *et al.*, Phys. Rev. Lett. **88**, 226803 (2002).
- [28] H. Haug and A.P. Jauho, *Quantum Kinetics in Transport and Optics of Semiconductors* (Springer, Berlin, 1996).